

# Strength of Nanotubes and Megacables

Nicola M. Pugno

**Abstract** In this chapter my findings [mainly reported in N. Pugno, *J. Phys.–Condens. Matter*, **18**, S1971–S1990 (2006); N. Pugno, *Acta Mater.* **55**, 5269–5279 (2007); N. Pugno, *Nano Today* **2**, 44–47 (2007)] on the mechanical strength of nanotubes and megacables are reviewed, with an eye to the challenging project of the carbon nanotube-based space elevator megacable. Accordingly, basing the design of the megacable on the theoretical strength of a single carbon nanotube, as originally proposed at the beginning of the third millennium, has been demonstrated to be naïve. The role on the fracture strength of thermodynamically unavoidable atomistic defects with different size and shape is thus here quantified on brittle fracture both numerically (with *ad hoc* hierarchical simulations) and theoretically (with quantized fracture theories), for nanotubes and nanotube bundles. Fatigue, elasticity, non-asymptotic regimes, elastic-plasticity, rough cracks, finite domains and size-effects are also discussed.

## Introduction

A space elevator basically consists of a cable attached to the Earth surface for carrying payloads into space [1]. If the cable is long enough, i.e. around 150 Mm (a value that can be reduced by a counterweight), the centrifugal forces exceed the gravity of the cable, that will work under tension [2]. The elevator would stay fixed geosynchronously; once sent far enough, climbers would be accelerated by the Earth's rotational energy. A space elevator would revolutionize the methodology for carrying payloads into space at low cost, but its design is very challenging. The most critical component in the space elevator design is undoubtedly the cable [3–5], that requires a material with very high strength and low density.

---

N.M. Pugno (✉)

Department of Structural Engineering and Geotechnics, Politecnico di Torino,  
Corso Duca degli Abruzzi 24, 10129 Torino, Italy  
e-mail: nicola.pugno@polito.it

Considering a cable with constant cross-section and a vanishing tension at the planet surface, the maximum stress-density ratio, reached at the geosynchronous orbit, is for the Earth equal to  $63 \text{ GPa}/(1,300 \text{ kg/m}^3)$ , corresponding to 63 GPa if the low carbon density is assumed for the cable. Only recently, after the re-discovery of carbon nanotubes [6], such a large failure stress has been experimentally measured, during tensile tests of ropes composed of single walled carbon nanotubes [7] or multiwalled carbon nanotubes [8] both expected to have an ideal strength of  $\sim 100 \text{ GPa}$ . Note that for steel (density of  $7,900 \text{ kg/m}^3$ , maximum strength of 5 GPa) the maximum stress expected in the cable would be of 383 GPa, whereas for kevlar (density of  $1,440 \text{ kg/m}^3$ , strength of 3.6 GPa) of 70 GPa, both much higher than their strengths [3].

However, an optimized cable design must consider a uniform tensile stress profile rather than a constant cross-section area [2]. Accordingly, the cable could be built of any material by simply using a large enough taper-ratio, that is the ratio between the maximum (at the geosynchronous orbit) and minimum (at the Earth's surface) cross-section area. For example, for steel or kevlar a giant and unrealistic taper-ratio would be required,  $10^{33}$  or  $2.6 \times 10^8$  respectively, whereas for carbon nanotubes it must theoretically be only  $1.9^9$ . Thus, the feasibility of the space elevator seems to become only currently plausible [9, 10] thanks to the discovery of carbon nanotubes. The cable would represent the largest engineering structure, hierarchically designed from the nano- (single nanotube with length of the order of a hundred nanometers) to the mega-scale (space elevator cable with a length of the order of a hundred megameters).

In this chapter the asymptotic analysis on the role of defects for the megacable strength, based on new theoretical deterministic and statistical approaches of quantized fracture mechanics proposed by the author [11–14], is extended to non asymptotic regimes, elastic-plasticity, rough cracks and finite domains. The role of thermodynamically unavoidable atomistic defects with different size and shape is thus quantified on brittle fracture, fatigue and elasticity, for nanotubes and nanotube bundles. The results are compared with atomistic and continuum simulations and nano-tensile tests of carbon nanotubes. Key simple formulas for the design of a flaw-tolerant space elevator megacable are reported, suggesting that it would need a taper-ratio (for uniform stress) of about two orders of magnitude larger than as today erroneously proposed.

The chapter is organized in 10 short sections, as follows. After this introduction, reported as the first section, we start calculating the strength of nanotube bundles by using *ad hoc* hierarchical simulations, discussing the related size-effect. In Sect. 'Brittle Fracture' the strength reduction of a single nanotube and of a nanotube bundle containing defects with given size and shape is calculated; the taper-ratio for a flaw-tolerant space elevator cable is accordingly derived. In Sect. 'Elastic-Plasticity, Fractal Cracks and Finite Domains' elastic-plastic (or hyper-elastic) materials, rough cracks and finite domains are discussed. In Sect. 'Fatigue' the fatigue life time is evaluated for a single nanotube and for a nanotube bundle. In Sect. 'Elasticity' the related Young's modulus degradations are quantified. In Sects. 'Atomistic Simulations', 'Nanotensile Tests' we compare our results on strength

and elasticity with atomistic simulations and tensile tests of carbon nanotubes. In Sect. ‘Thermodynamic Limit’ we demonstrate that defects are thermodynamically unavoidable, evaluating the minimum defect size and corresponding maximum achievable strength. The last section presents our concluding remarks.

## Hierarchical Simulations and Size-Effects

To evaluate the strength of carbon nanotube cables, the SE<sup>3</sup> algorithm, formerly proposed [3] has been adopted [15]. Multiscale simulations are necessary in order to tackle the size scales involved, spanning over  $\sim 10$  orders of magnitude from nanotube length ( $\sim 100$  nm) to kilometre-long cables, and also to provide useful information about cable scaling properties with length.

The cable is modelled as an ensemble of stochastic ‘springs’, arranged in parallel sections. Linearly increasing strains are applied to the fibre bundle, and at each algorithm iteration the number of fractured springs is computed (fracture occurs when local stress exceeds the nanotube failure strength) and the strain is uniformly redistributed among the remaining intact springs in each section.

In-silico stress-strain experiments have been carried out according to the following hierarchical architecture. Level 1: the nanotubes (single springs, Level 0) are considered with a given elastic modulus and failure strength distribution and composing a  $40 \times 1,000$  lattice or fibre. Level 2: again a  $40 \times 1,000$  lattice composed by second level ‘springs’, each of them identical to the entire fibre analysed at the first level, is analysed with in input the elastic modulus and stochastic strength distribution derived as the output of the numerous simulations to be carried out at the first level. And so on. Five hierarchical levels are sufficient to reach the size-scale of the megametre from that of the nanometre, Fig. 1.

The level 1 simulation is carried out with springs  $L_0 = 10^{-7}$  m in length,  $w_0 = 10^{-9}$  m in width, with Young’s modulus  $E_0 = 10^{12}$  Pa and strength  $\sigma_f$  randomly distributed according to the nanoscale Weibull statistics [16]  $P(\sigma_f) = 1 - \exp[-(\sigma_f/\sigma_0)^m]$ , where  $P$  is the cumulative probability. Fitting to experiments [7, 8], we have derived for carbon nanotubes  $\sigma_0 = 34$  GPa and  $m = 2.7$  [16]. Then the level 2 is computed, and so on. The results are summarized in Fig. 2, in which a strong size-effect is observed, up to length of  $\sim 1$  m.

Given the decaying  $\sigma_f$  vs. cable length  $L$  obtained from simulations, it is interesting to fit the behaviour with simple analytical scaling laws. Various exist in the literature, and one of the most used is the Multi-Fractal Scaling Law (MFSL [17], see also [18]) proposed by Carpinteri. This law has been recently extended towards the nanoscale [19]:

$$\frac{\sigma_f}{\sigma_{macro}} = \sqrt{1 + \frac{l_{ch}}{L + l_0}} \quad (1)$$

where  $\sigma_f$  is the failure stress,  $\sigma_{macro}$  is the macrostrength,  $L$  is the structural characteristic size,  $l_{ch}$  is a characteristic internal length and  $l_0$  is defined via

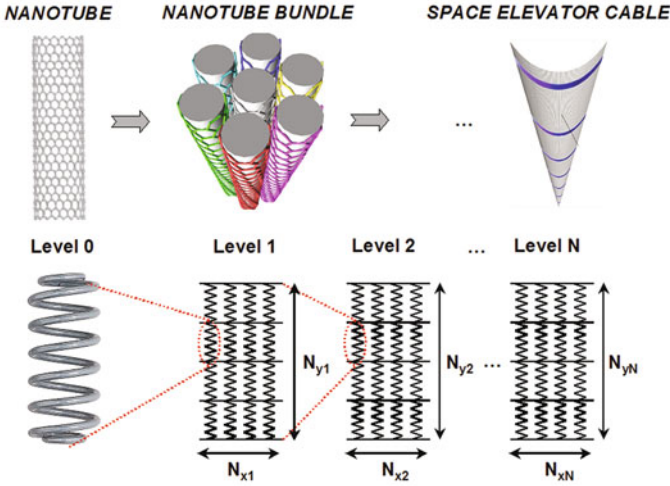


**Fig. 1** Schematization of the adopted multiscale simulation procedure to determine the space elevator cable strength. Here,  $N = 5$ ,  $N_{x1} = N_{x2} = \dots N_{x5} = 40$  and  $N_{y1} = N_{y2} = \dots N_{y5} = 1,000$ , so that the total number of nanotubes in the space elevator cable is  $N_{tot} = (1,000 \times 40)^5 \approx 10^{23}$  [15]

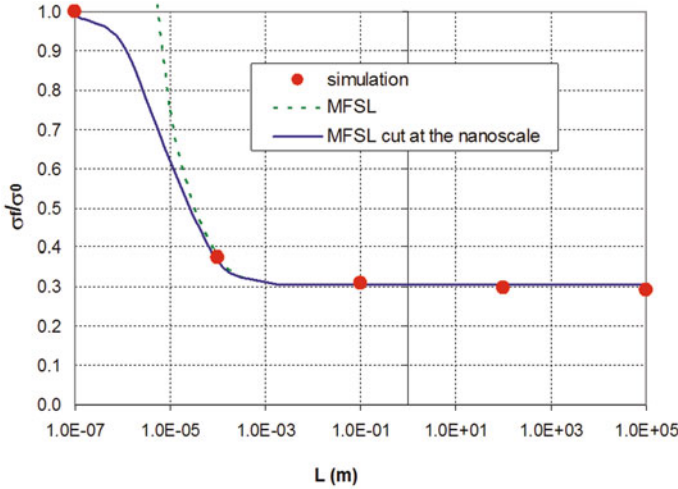


**Fig. 2** Comparison between simulations and analytical scaling law Eq. 1 for the failure strength of the nanotube bundle as a function of its length; the asymptote is at 10.20 GPa [15]

$\sigma_f(l=0) = \sigma_{macro} \sqrt{1 + \frac{l_{ch}}{l_0}} \equiv \sigma_{nano}$ , where  $\sigma_{nano}$  is the nanostrength. Note that for  $l_0 = 0$  this law is identical to the Carpinteri' scaling law [17]. Here, we can choose  $\sigma_{nano}$  as the nanotube stochastic strength, i.e.  $\sigma_{nano} = 34$  GPa. The computed macrostrength is  $\sigma_{macro} = 10.20$  GPa. The fit with Eq. 1 is shown in

Fig. 1 ('MFSL cut at the nanoscale'), for the various  $L$  considered at the different hierarchical levels (and compared with the classical 'MFSL'). The best fit is obtained for  $l_{ch} = 5 \times 10^{-5}$  m, where the analytical law is practically coincident with the simulated results. Thus, for a carbon nanotube megacable we have numerically derived a plausible strength  $\sigma_C = \sigma_{macro} \approx 10$  GPa.

## Brittle Fracture

By considering Quantized Fracture Mechanics (QFM; [11–14]), the failure stress  $\sigma_N$  for a nanotube having atomic size  $q$  (the 'fracture quantum') and containing an elliptical hole of half-axes  $a$  perpendicular to the applied load (or nanotube axis) and  $b$  can be determined including in the asymptotic solution [12] the contribution of the far field stress. We accordingly derive:

$$\frac{\sigma_N(a, b)}{\sigma_N^{(theo)}} = \sqrt{\frac{1 + 2a/q(1 + 2a/b)^{-2}}{1 + 2a/q}}, \quad \sigma_N^{(theo)} = \frac{K_{IC}}{\sqrt{q\pi/2}} \quad (2)$$

where  $\sigma_N^{(theo)}$  is the theoretical (defect-free) nanotube strength ( $\sim 100$  GPa, see Table 1) and  $K_{IC}$  is the material fracture toughness. The self-interaction between the tips has been here neglected (i.e.  $a \ll \pi R$ , with  $R$  nanotube radius) and would further reduce the failure stress. For atomistic defects (having characteristic length of few Ångstrom) in nanotubes (having characteristic diameter of several nanometers) this hypothesis is fully verified. However, QFM can easily treat also the self-tip interaction starting from the corresponding value of the stress-intensity factor (reported in the related Handbooks). The validity of QFM has been recently confirmed by atomistic simulations [3–5, 12, 13, 20], but also at larger size-scales [12, 13, 21] and for fatigue crack growth [14, 22, 23].

**Table 1** Atomistic simulations [30–33] vs. QFM predictions, for nano-cracks of size  $n$  or nano-holes of size  $m$  [4]

Nanotube type	Nanocrack ( $n$ ) and nanohole ( $m$ ) sizes	Strength (GPa) by QM (MTB-G2) and MM (PM3; M) QM/MM atomistic or QFM calculations
[5, 5]	Defect-free	105 (MTB-G2); 135 (PM3)
[5, 5]	$n = 1$ (Sym.+H)	85 (MTB-G2), 79 (QFM); 106 (PM3), 101 (QFM)
[5, 5]	$n = 1$ (Asym.+H)	71 (MTB-G2), 79 (QFM); 99 (PM3), 101 (QFM)
[5, 5]	$n = 1$ (Asym.)	70 (MTB-G2), 79 (QFM); 100 (PM3), 101 (QFM)
[5, 5]	$n = 2$ (Sym.)	71 (MTB-G2), 63 (QFM); 105 (PM3), 81 (QFM)
[5, 5]	$n = 2$ (Asym.)	73 (MTB-G2), 63 (QFM); 111 (PM3), 81 (QFM)
[5, 5]	$m = 1$ (+H)	70 (MTB-G2), 68 for long tube, 79 (QFM); 101 (PM3), 101 (QFM)
[5, 5]	$m = 2$ (+H)	53 (MTB-G2), 50 for long tube, 67 (QFM); 78 (PM3), 86 (QFM)

**Table 1** (continued)

Nanotube type	Nanocrack ( $n$ ) and nanohole ( $m$ ) sizes	Strength (GPa) by QM (MTB-G2) and MM (PM3; M) QM/MM atomistic or QFM calculations
[10, 10]	Defect-free	88 (MTB-G2); 124 (PM3)
[10, 10]	$n = 1$ (sym.+H)	65 (MTB-G2), 66 (QFM)
[10, 10]	$n = 1$ (Asym.+H)	68 (MTB-G2), 66 (QFM)
[10, 10]	$n = 1$ (Sym.)	65 (MTB-G2), 66 (QFM); 101 (PM3), 93 (QFM)
[10, 10]	$n = 2$ (Sym.)	64 (MTB-G2), 53 (QFM); 107 (PM3), 74 (QFM)
[10, 10]	$n = 2$ (Asym.)	65 (MTB-G2), 53 (QFM); 92 (PM3), 74 (QFM)
[10, 10]	$m = 1$ (+H)	56 (MTB-G2), 52 for long tube, 66 (QFM); 89 (PM3), 93 (QFM)
[10, 10]	$m = 2$ (+H)	42 (MTB-G2), 36 for long tube, 56 (QFM); 67 (PM3), 79 (QFM)
[50, 0]	Defect-free	89 (MTB-G2)
[50, 0]	$m = 1$ (+H)	58 (MTB-G2); 67 (QFM)
[50, 0]	$m = 2$ (+H)	46 (MTB-G2); 57 (QFM)
[50, 0]	$m = 3$ (+H)	40 (MTB-G2); 44 (QFM)
[50, 0]	$m = 4$ (+H)	36 (MTB-G2); 41 (QFM)
[50, 0]	$m = 5$ (+H)	33 (MTB-G2); 39 (QFM)
[50, 0]	$m = 6$ (+H)	31 (MTB-G2); 37 (QFM)
[100, 0]	Defect-free	89 (MTB-G2)
[100, 0]	$m = 1$ (+H)	58 (MTB-G2); 67 (QFM)
[100, 0]	$m = 2$ (+H)	47 (MTB-G2); 57 (QFM)
[100, 0]	$m = 3$ (+H)	42 (MTB-G2); 44 (QFM)
[100, 0]	$m = 4$ (+H)	39 (MTB-G2); 41 (QFM)
[100, 0]	$m = 5$ (+H)	37 (MTB-G2); 39 (QFM)
[100, 0]	$m = 6$ (+H)	35 (MTB-G2); 37 (QFM)
[29, 29]	Defect-free	101 (MTB-G2)
[29, 29]	$m = 1$ (+H)	77 (MTB-G2); 76 (QFM)
[29, 29]	$m = 2$ (+H)	62 (MTB-G2); 65 (QFM)
[29, 29]	$m = 3$ (+H)	54 (MTB-G2); 50 (QFM)
[29, 29]	$m = 4$ (+H)	48 (MTB-G2); 46 (QFM)
[29, 29]	$m = 5$ (+H)	45 (MTB-G2); 44 (QFM)
[29, 29]	$m = 6$ (+H)	42 (MTB-G2); 42 (QFM)
[47, 5]	Defect-free	89 (MTB-G2)
[47, 5]	$m = 1$ (+H)	57 (MTB-G2); 67 (QFM)
[44, 10]	Defect-free	89 (MTB-G2)
[44, 10]	$m = 1$ (+H)	58 (MTB-G2); 67 (QFM)
[40, 16]	Defect-free	92 (MTB-G2)
[40, 16]	$m = 1$ (+H)	59 (MTB-G2); 69 (QFM)
[36, 21]	Defect-free	96 (MTB-G2)
[36, 21]	$m = 1$ (+H)	63 (MTB-G2); 72 (QFM)
[33, 24]	Defect-free	99 (MTB-G2)
[33, 24]	$m = 1$ (+H)	67 (MTB-G2); 74 (QFM)

**Table 1** (continued)

Nanotube type	Nanocrack ( $n$ ) and nanohole ( $m$ ) sizes	Strength (GPa) by QM (MTB-G2) and MM (PM3; M) QM/MM atomistic or QFM calculations
[80, 0]	Defect-free	93 (M)
[80, 0]	$n = 2$	64 (M); 56 (QFM)
[80, 0]	$n = 4$	50 (M); 43 (QFM)
[80, 0]	$n = 6$	42 (M); 35 (QFM)
[80, 0]	$n = 8$	37 (M); 32 (QFM)
[40, 0] (nested by a [32, 0])	Defect-free	99 (M)
[40, 0] (nested by a [32, 0])	$n = 2$	73 (M); 69 (QFM + vdW interaction $\sim 10$ GPa)
[40, 0] (nested by a [32, 0])	$n = 4$	57 (M); 56 (QFM + vdW interaction $\sim 10$ GPa)
[40, 0] (nested by a [32, 0])	$n = 6$	50 (M); 48 (QFM + vdW interaction $\sim 10$ GPa)
[40, 0] (nested by a [32, 0])	$n = 8$	44 (M); 44 (QFM + vdW interaction $\sim 10$ GPa)
[100, 0]	Defect-free	89 (MTB-G2)
[100, 0]	$n = 4$	50 (M); 41 (QFM)
[10, 0]	Defect free	124 (QM); 88 (MM);
[10, 0]	$n = 1$	101 (QM) 95 (QM/MM) 93 (QFM); 65 (MM) 66 (QFM)

The QFM predictions are here obtained simply considering in Eq. 2  $2a/q = n$ ,  $2b/q = 1$  for cracks of size  $n$  or  $a/q = b/q = (2m - 1)/\sqrt{3}$  for holes of size  $m$ . Quantum mechanics (QM) semi-empirical calculations (PM3 method), Molecular Mechanics (MM) calculations (modified Tersoff-Brenner potential of second generation (MTB-G2), modified Morse potential (M) and coupled QM/MM calculations. The symbol (+H) means that the defect was saturated with hydrogen. Symmetric and asymmetric bond reconstructions were also considered; the tubes are 'short', if not otherwise specified. We have roughly ignored in the QFM predictions the difference between symmetric and asymmetric bond reconstruction, hydrogen saturation and length-effect (for shorter tubes an increment in the strength is always observed, as an intrinsic size-effect), noting that the main differences in the atomistic simulations are imputable to the used potential. For nested nanotubes a strength increment of  $\sim 10$  GPa is here assumed to roughly take into account the van der Waals (vdW) interaction between the walls

Regarding the defect shape, for a sharp crack perpendicular to the applied load  $a/q = \text{const}$  &  $b/q \rightarrow 0$ , thus  $\sigma_N \approx \sigma_N^{(theo)}/\sqrt{1 + 2a/q}$ , and for  $a/q \gg 1$ , i.e. large cracks,  $\sigma_N \approx K_{IC}/\sqrt{\pi a}$  in agreement with Linear Elastic Fracture Mechanics (LEFM); note that LEFM can (1) only treat sharp cracks and (2) unreasonably predicts an infinite defect-free strength. On the other hand, for a crack parallel to the applied load  $b/q = \text{const}$  &  $a/q \rightarrow 0$  and thus  $\sigma_N = \sigma_N^{(theo)}$ , as it must be. In addition, regarding the defect size, for self-similar and small holes  $a/b = \text{const}$  &  $a/q \rightarrow 0$  and coherently  $\sigma_N = \sigma_N^{(theo)}$ ; furthermore, for self-similar and large holes  $a/b = \text{const}$  &  $a/q \rightarrow \infty$  and we deduce  $\sigma_N \approx \sigma_N^{(theo)}/(1 + 2a/b)$  in agreement with the stress-concentration posed by Elasticity; but Elasticity (coupled with a

maximum stress criterion) unreasonably predicts (3) a strength independent from the hole size and (4) tending to zero for cracks. Note the extreme consistency of Eq. 2, that removing all the limitations (1–4) represents the first law capable of describing in a unified manner all the size- and shape-effects for the elliptical holes, including cracks as limit case. In other words, Eq. 2 shows that the two classical strength predictions based on stress-intensifications (LEFM) or -concentrations (Elasticity) are only reasonable for ‘large’ defects; Eq. 2 unifies their results and extends its validity to ‘small’ defects (‘large’ and ‘small’ are here with respect to the fracture quantum). Eq. 2 shows that even a small defect can dramatically reduces the mechanical strength.

An upper bound of the cable strength can be derived assuming the simultaneous failure of all the defective nanotubes present in the bundle. Accordingly, imposing the critical force equilibrium (mean-field approach) for a cable composed by nanotubes in numerical fractions  $f_{ab}$  containing holes of half-axes  $a$  and  $b$ , we find the cable strength  $\sigma_C$  (ideal if  $\sigma_C^{(theo)}$ ) in the following form:

$$\frac{\sigma_C}{\sigma_C^{(theo)}} = \sum_{a,b} f_{ab} \frac{\sigma_N(a,b)}{\sigma_N^{(theo)}} \quad (3)$$

The summation is extended to all the different holes; the numerical fraction  $f_{00}$  of nanotubes is defect-free and  $\sum_{a,b} f_{ab} = 1$ . If all the defective nanotubes in the bundle contain identical holes  $f_{ab} = f = 1 - f_{00}$ , and the following simple relation between the strength reductions holds:  $1 - \sigma_C/\sigma_C^{(theo)} = f \left(1 - \sigma_N/\sigma_N^{(theo)}\right)$ .

Thus, the taper-ratio  $\lambda$  needed to have a uniform stress in the cable [2], under the centrifugal and gravitational forces, must be larger than its theoretical value to design a flaw-tolerant megacable. In fact, according to our analysis, we deduce ( $\lambda = e^{const \cdot \rho_C/\sigma_C} \geq \lambda^{(theo)} \approx 1.9$  for carbon nanotubes;  $\rho_C$  denotes the material density):

$$\frac{\lambda}{\lambda^{(theo)}} = \lambda^{(theo)} \left( \frac{\sigma_C^{(theo)}}{\sigma_C} - 1 \right) \quad (4)$$

Equation 4 shows that a small defect can dramatically increase the taper-ratio required for a flaw-tolerant megacable.

## Elastic-Plasticity, Fractal Cracks and Finite Domains

The previous equations are based on linear elasticity, i.e., on a linear relationship  $\sigma \propto \varepsilon$  between stress  $\sigma$  and strain  $\varepsilon$ . In contrast, let us assume  $\sigma \propto \varepsilon^\kappa$ , where  $\kappa > 1$  denotes hyper-elasticity, as well as  $\kappa < 1$  elastic-plasticity. The power of the stress-singularity will accordingly be modified [24] from the classical value 1/2 to



$\alpha = \kappa / (\kappa + 1)$ . Thus, the problem is mathematically equivalent to that of a re-entrant corner [25], and consequently we predict:

$$\frac{\sigma_N(a, b, \alpha)}{\sigma_N^{(theo)}} = \left( \frac{\sigma_N(a, b)}{\sigma_N^{(theo)}} \right)^{2\alpha}, \quad \alpha = \frac{\kappa}{\kappa + 1} \quad (5)$$

A crack with a self-similar roughness, mathematically described by a fractal with non-integer dimension  $1 < D < 2$ , would similarly modify the stress-singularity, according to [18, 26]  $\alpha = (2 - D)/2$ ; thus, with Eq. 5, we can also estimate the role of the crack roughness. Both plasticity and roughness reduce the severity of the defect, whereas hyper-elasticity enlarges its effect. For example, for a crack composed by  $n$  adjacent vacancies, we found  $\sigma_N / \sigma_N^{(theo)} \approx (1 + n)^{-\alpha}$ .

However, note that among these three effects only elastic-plasticity may have a significant role in carbon nanotubes; in spite of this, fractal cracks could play an important role in nanotube bundles as a consequence of their larger size-scale, which would allow the development of a crack surface roughness. Hyper-elasticity is not expected to be relevant in this context.

According to LEFM and assuming the classical hypothesis of self-similarity ( $a_{\max} \propto L$ ), i.e., the largest crack size is proportional to the characteristic structural size  $L$ , we expect a size-effect on the strength in the form of the power law  $\sigma_C \propto L^{-\alpha}$ . For linear elastic materials  $\alpha = 1/2$  as classically considered, but for elastic-plastic materials or fractal cracks  $0 \leq \alpha \leq 1/2$  [24], whereas for hyper-elastic materials  $1/2 \leq \alpha \leq 1$ , suggesting an unusual and super-strong size-effect. This parameter would represent the maximum slope (in a bi-log plot) of the scaling reported in Fig. 1.

Equation 2 does not consider the defect-boundary interaction. The finite width  $2W$ , can be treated by applying QFM starting from the related expression of the stress-intensity factor (reported in Handbooks). However, to have an idea of the defect-boundary interaction, we apply an approximated method [27], deriving the following correction  $\sigma_N(a, b, W) \approx C(W) \sigma_N(a, b)$ ,  $C(W) \approx (1 - a/W) / \left( \sigma_N(a, b) \Big|_{q \rightarrow W-a} / \sigma_N^{(theo)} \right)$  (note that such a correction is valid also for  $W \approx a$ , whereas for  $W \gg a$  it becomes  $C(W \gg a) \approx 1 - a/W$ ). Similarly, the role of the defect orientation  $\beta$  could be treated by QFM considering the related stress-intensity factor; roughly, one could use the self-consistent approximation  $\sigma_N(a, b, \beta) \approx \sigma_N(a, b) \cos^2 \beta + \sigma_N(b, a) \sin^2 \beta$ .

## Fatigue

The space elevator cable will be cyclically loaded, e.g., by the climbers carrying the payloads, thus fatigue could play a role on its design. By integrating the quantized Paris' law, that is an extension of the classical Paris' law recently proposed

especially for nanostructure or nanomaterial applications [14, 22, 23], we derive the following number of cycles to failure (or life time):

$$\frac{C_N(a)}{C_N^{(theo)}} = \frac{(1 + q/W)^{1-m/2} - (a/W + q/W)^{1-m/2}}{(1 + q/W)^{1-m/2} - (q/W)^{1-m/2}}, \quad m \neq 2 \quad (6a)$$

$$\frac{C_N(a)}{C_N^{(theo)}} = \frac{\ln \{(1 + q/W) / (a/W + q/W)\}}{\ln \{(1 + q/W) / (q/W)\}}, \quad m = 2 \quad (6b)$$

where  $m > 0$  is the material Paris' exponent. Note that according to Wöhler  $C_N^{(theo)} = K \Delta \sigma^{-k}$ , where  $K$  and  $k$  are material constants and  $\Delta \sigma$  is the amplitude of the stress range during the oscillations. Even if fatigue experiments in nanotubes are still to be performed, their behaviour is expected to be intermediate between those of Wöhler and Paris, as displayed by all the known materials, and the quantized Paris' law basically represents their asymptotic matching (as quantized fracture mechanics basically represents the asymptotic matching between the strength and toughness approaches).

Only defects remaining self-similar during fatigue growth have to be considered, thus only a crack (of half-length  $a$ ) is of interest in this context. By means of Eq. 6 the time to failure reduction can be estimated, similarly to the brittle fracture treated by Eq. 2.

For a bundle, considering a mean-field approach (similarly to Eq. 3) yields:

$$\frac{C_C}{C_C^{(theo)}} = \sum_a f_a \frac{C_N(a)}{C_N^{(theo)}} \quad (7)$$

Better predictions could be derived integrating the quantized Paris' law for a finite width strip. However, we note that the role of the finite width is already included in Eq. 6, even if these are rigorously valid in the limit of  $W$  tending to infinity.

## Elasticity

Consider a nanotube of lateral surface  $A$  under tension and containing a transversal crack of half-length  $a$ . Interpreting the incremental compliance, due to the presence of the crack, as a Young's modulus (here denoted by  $E$ ) degradation we find  $\frac{E(a)}{E^{(theo)}} = 1 - 2\pi \frac{a^2}{A}$  [28]. Thus, recursively, considering  $Q$  cracks (in the megacable  $10^{12} - 10^{20}$  defects are expected, see Sect. 'Hierarchical Simulations and Size-Effects') having sizes  $a_i$  or, equivalently,  $M$  different cracks with multiplicity  $Q_i$  ( $Q = \sum_{i=1}^M Q_i$ ), noting that  $n_i = \frac{2a_i}{q}$  represents the number of adjacent vacancies in a crack of half-length  $a_i$ , with  $q$  atomic size, and  $v_i = \frac{Q_i n_i}{A/q^2}$  its related numerical (or volumetric) vacancy fraction, we find [28]:

$$\frac{E}{E^{(theo)}} = \prod_{i=1}^Q \frac{E(a_i)}{E^{(theo)}} \approx 1 - \xi \sum_{i=1}^M v_i n_i \quad (8)$$

with  $\xi \geq \pi/2$ , where the equality holds for isolated cracks. Eq. 8 can be applied to nanotubes or nanotube bundles containing defects in volumetric percentages  $v_i$ .

Forcing the interpretation of our formalism, we note that  $n_i = 1$  would describe a single vacancy, i.e., a small hole. Thus, as a first approximation, different defect geometries, from cracks to circular holes, e.g., elliptical holes, could in principle be treated by Eq. 8; we have to interpret  $n_i$  as the ratio between the transversal and longitudinal (parallel to the load) defect sizes ( $n_i = a_i/b_i$ ). Introducing the  $i$ -th defect eccentricity  $e_i$  as the ratio between the lengths of the longer and shorter axes, as a first approximation  $n_i(\beta_i) \approx e_i \cos^2 \beta_i + 1/e_i \sin^2 \beta_i$ , where  $\beta_i$  is the defect orientation. For a single defect typology  $\frac{E}{E^{(theo)}} \approx 1 - \xi v n$ , in contrast to the common assumption  $\frac{E}{E^{(theo)}} \approx 1 - v$ , rigorously valid only for the cable density, for which  $\frac{\rho_C}{\rho_C^{(theo)}} \equiv 1 - v$ . Note that the failure strain for a defective nanotube or nanotube

bundle can also be predicted, by  $\varepsilon_{N,C}/\varepsilon_{N,C}^{(theo)} = \left( \sigma_{N,C}/\sigma_{N,C}^{(theo)} \right) / \left( E/E^{(theo)} \right)$ .

In contrast to what happens for the strength, large defectiveness is required to have a considerable elastic degradation, even if we have shown that sharp transversal defects could have a role. For example, too soft space elevator cables would become dynamically unstable [29].

## Atomistic Simulations

Let us study the influence on the strength of nano-cracks and circular nano-holes.  $n$  atomic adjacent vacancies perpendicular to the load, correspond to a blunt nano-crack of length  $2a \approx nq$  and thickness  $2b \approx q$  (or  $2a \approx nq$  with a radius at tips of  $b^2/a \approx q/2$ ). Similarly, nano-holes of size  $m$  can be considered: the index  $m=1$  corresponds to the removal of an entire hexagonal ring,  $m=2$  to the additional removal of the six hexagons around the former one (i.e. the adjacent perimeter of 18 atoms),  $m=3$  to the additional removal of the neighbouring 12 hexagonal rings (next adjacent perimeter), and so on (thus  $a = b \approx q(2m-1)/\sqrt{3}$ ). Quantum mechanics (QM), semi-empirical (PM3 method), Molecular Mechanics (MM; with a modified Tersoff-Brenner potential of second generation (MTB-G2) or a modified Morse potential (M)) and coupled QM/MM calculations [30–33] are reported and extensively compared in Table 1 with the QFM non-asymptotic predictions of Eq. 2 (differently from the asymptotic comparison reported in [3, 12]). The comparison shows a relevant agreement, confirming and demonstrating that just a few vacancies can dramatically reduce the strength of a single nanotube, or of a nanotube bundle as described by Eq. 3 that predicts for  $f \approx 1$ ,  $\sigma_C/\sigma_C^{(theo)} \approx \sigma_N/\sigma_N^{(theo)}$ . Assuming large holes ( $m \rightarrow \infty$ ) and applying QFM to a defective bundle ( $f \approx 1$ ), we predict  $1 - \sigma_C/\sigma_C^{(theo)} \approx 1 - \sigma_N/\sigma_N^{(theo)} \approx 67\%$ ; but nano-cracks surely would be even

more critical, especially if interacting with each other or with the boundary. Thus, the expectation for the megacable of a strength larger than  $\sim 33$  GPa is unrealistic.

Note that an elastic ( $\kappa \approx 1$ ) nearly perfectly plastic ( $\kappa \approx 0$ ) behaviour, with a flow stress at  $\sim 30$ – $35$  GPa for strains larger than  $\sim 3$ – $5\%$ , has been recently observed in tensile tests of carbon nanotubes [34], globally suggesting  $\kappa \approx 0.6 - 0.7$ ; similarly, numerically computed stress-strain curves [35] reveal for an armchair (5, 5) carbon nanotube  $\kappa \approx 0.8$ , whereas for a zig-zag (9, 0) nanotube  $\kappa \approx 0.7$ , suggesting that the plastic correction reported in Sect. ‘Elastic-Plasticity, Fractal Cracks and Finite Domains’ could have a role.

Regarding elasticity, we note that Eq. 8 can be viewed as a generalization of the approach proposed in [36], being able to quantify the constants  $k_i$  fitted by atomistic simulations for three different types of defect [28]. In particular, rearranging Eq. 8 and in the limit of three small cracks, we deduce  $\frac{E_{th}}{E} \approx 1 + k_1 c_1 + k_2 c_2 + k_3 c_3$ , identical to their law (their Eq. 15), in which  $c_i = Q_i/L$  is the linear defect concentration in a nanotube of length  $L$  and radius  $R$  and  $k_i = \frac{\xi c_i n_i^2 q^2}{\pi^2 R}$ . These authors consider 1, 2 and 3 atoms missing, with and without reconstructed bonds; for non-reconstructed bonds two alternative defect orientations were investigated for 2 and 3 atoms missing. Even if their defect geometries are much more complex than the nanocracks that we here consider, the comparison between our approach and their atomistic simulations, which does not involve best-fit parameters, shows a good agreement [28].

## Nanotensile Tests

The discussed tremendous defect sensitivity, described by Eq. 2, is confirmed by a statistical analysis based on Nanoscale Weibull Statistics [16] applied to the nanotensile tests. According to this treatment, the probability of failure  $P$  for a nearly defect-free nanotube under a tensile stress  $\sigma_N$  is independent from its volume (or surface), in contrast to classical Weibull Statistics [37], namely:

$$P = 1 - \exp -N_N \left( \frac{\sigma_N}{\sigma_0} \right)^w \quad (9)$$

where  $w$  is the nanoscale Weibull modulus,  $\sigma_0$  is the nominal failure stress (i.e. corresponding to a probability of failure of 63%) and  $N_N \equiv 1$ . In classical Weibull statistics  $N_N \equiv V/V_0$  for volume dominating defects (or  $N_N = A/A_0$  for surface dominating defects), i.e.,  $N_N$  is the ratio between the volume (or surface) of the structure and a reference volume (or surface). The experimental data on carbon nanotubes [7, 8] were treated [16] according to nanoscale and classical Weibull statistics: the coefficients of correlation were found to be much higher for the nanoscale statistics than for the classical one (0.93 against 0.67,  $w \approx 2.7$  and  $\sigma_0 \approx 31 - 34$  GPa). The data set on MWCNT tensile experiments [38] has also been statistically treated [3]. The very large highest measured strengths denotes interactions between the external and internal walls, as pointed out by the same authors [38] and recently quantified [14]. Thus, the measured strengths cannot be

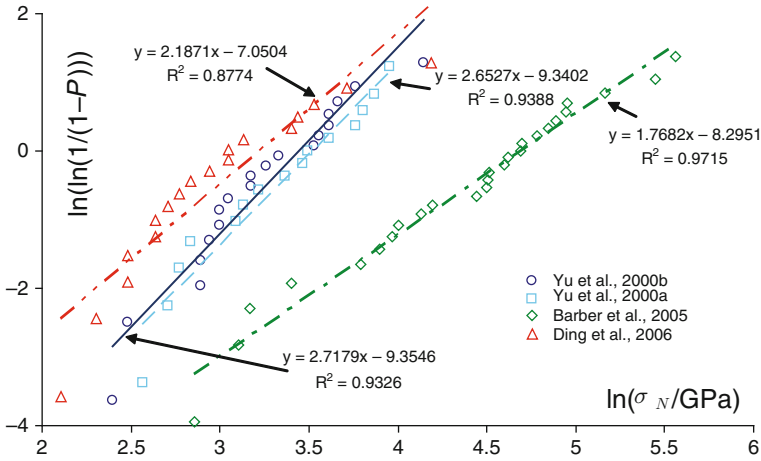


**Fig. 3** Nanoscale Weibull Statistics, straight lines, applied to the new nanotensile experiments on carbon nanotubes [4]

considered plausible for describing the strength of a SWCNT. Such experiments were best-fitted with  $\sigma_0 \approx 108$  GPa (but not significant for the strength of a single nanotube) and  $w \approx 1.8$  (coefficient of correlation 0.94). In Fig. 3, the new data set [39] is treated [4] by applying NWS ( $N_N \equiv 1$ ,  $w \approx 2.2$ ,  $\sigma_0 \approx 25$  GPa) and compared with the other nanoscale statistics [3, 4] deduced from the other data sets [7, 8, 38]. Note that volume- or surface-based Weibull statistics are identical in treating the external wall of the tested nanotubes, just an atomic layer thick. We have found a poor coefficient of correlation also treating this new data set with classical Weibull statistics, namely 0.51 (against 0.88 for NWS, see Fig. 3).

All these experimental data [7, 8, 38, 39] are treated in Table 2, by applying QFM in the form of Eq. 2: non-linear multiple solutions for identifying the defects corresponding to the measured strength clearly emerge; however these are quantifiable, showing that a small defect is sufficient to rationalize the majority of the observed strong strength reductions.

Finally, the new experimental results [38] are differently treated in Table 3, with respect to both strength and elasticity, assuming the presence of transversal nano-cracks. The ideal strength is assumed to be of 100 GPa and the theoretical Young's modulus of 1 TPa; by Eq. 2 the crack length  $n$  is calculated and introduced in Eq. 8 to derive the related vacancy fraction  $v$  ( $\xi = \pi/2$ ).

## Thermodynamic Limit

Defects are thermodynamically unavoidable, especially at the megascale. At the thermal equilibrium the vacancy fraction  $f = n/N \ll 1$  ( $n$  is the number of vacancies and  $N$  is the total number of atoms) is estimated as [40]:

$$f \approx e^{-E_1/k_B T_a} \quad (10)$$

**Table 2** Experiments vs. QFM predictions; strength reduction  $\sigma_N(a, b)/\sigma_N^{(theo)}$  derived according to Eq. 2 [4]

$\sigma_N/\sigma_N^{(theo)}$ $2b/q$	0	1	2	3	4	5	6	7	8	9	10	$\infty$
0	1.00*	1.00*	1.00*	1.00*	1.00*	1.00*	1.00*	1.00*	1.00*	1.00*	1.00*	1.00
1	0.71*	0.75	0.79	0.82	0.85	0.87*	0.88*	0.90	0.91	0.91	0.92	1.00
2	0.58	0.60*	0.64*	0.68	0.71*	0.73	0.76	0.78*	0.79	0.81	0.82	1.00
3	0.50	<b>0.52</b>	0.54*	0.58	0.61	0.64*	<u>0.66*</u>	0.68	0.70*	0.72	0.74	1.00
4	<b>0.45</b>	0.46	<b>0.48</b>	0.51*	0.54*	0.56	0.59	0.61	0.63	0.65	0.67	1.00
5	<u>0.41</u>	0.42	0.44*	0.46	<b>0.48</b>	0.51*	0.53*	0.55*	0.58	0.59	0.61	1.00
6	0.38	0.38	0.40	0.42	0.44*	0.47	0.49*	0.51*	0.53*	0.55*	0.57	1.00
7	0.35	0.36	<u>0.37</u>	<u>0.39</u>	<u>0.41</u>	<b>0.43</b>	<b>0.45</b>	0.47	0.49*	0.51*	0.53*	1.00
8	<b>0.33</b>	<u>0.34</u>	0.35	<u>0.37</u>	0.38	0.40	0.42	0.44*	0.46	<b>0.48</b>	0.49*	1.00
9	<b>0.32</b>	<b>0.32</b>	<b>0.33</b>	<u>0.34</u>	0.36	0.38	0.40	0.41	<b>0.43</b>	<b>0.45</b>	0.46	1.00
10	<u>0.30*</u>	<u>0.30*</u>	<u>0.31</u>	<b>0.33</b>	<u>0.34</u>	0.36	<u>0.37</u>	<u>0.39</u>	<u>0.41</u>	0.42	0.44*	1.00
11	<b>0.29</b>	<b>0.29</b>	<u>0.30*</u>	<u>0.31</u>	<b>0.32</b>	<u>0.34</u>	0.35	<b>0.37</b>	<u>0.39</u>	0.40	0.42	1.00
12	0.28	0.28	<b>0.29</b>	<u>0.30*</u>	<u>0.31</u>	<b>0.32</b>	<u>0.34</u>	0.35	<b>0.37</b>	0.38	0.40	1.00
13	0.27	0.27	0.28	<b>0.29</b>	<u>0.30*</u>	<u>0.31</u>	<b>0.32</b>	<u>0.34</u>	0.35	0.36	0.38	1.00
14	0.26	0.26	0.27	0.27	<b>0.29</b>	<u>0.30*</u>	<u>0.31</u>	<b>0.32</b>	<u>0.34</u>	0.35	0.36	1.00
15	<b>0.25</b>	<b>0.25</b>	0.26	0.27	0.27	<b>0.29</b>	<u>0.30*</u>	<u>0.31</u>	<b>0.32</b>	<u>0.34</u>	0.35	1.00
16	0.24*	0.24*	<b>0.25</b>	0.26	0.27	0.28	<b>0.29</b>	<u>0.30*</u>	<u>0.31</u>	0.32	<b>0.33</b>	1.00
17	0.24*	0.24*	0.24*	<b>0.25</b>	0.26	0.27	0.28	<b>0.29</b>	<u>0.30*</u>	<u>0.31</u>	<b>0.32</b>	1.00
18	<b>0.23</b>	<b>0.23</b>	0.24*	0.24*	<b>0.25</b>	0.26	0.27	0.28	<b>0.29</b>	<u>0.30*</u>	<u>0.31</u>	1.00
19	<u>0.22*</u>	<u>0.22*</u>	<b>0.23</b>	<b>0.23</b>	0.24*	<b>0.25</b>	0.26	0.27	0.28	<b>0.29</b>	<u>0.30*</u>	1.00
20	<u>0.22*</u>	<u>0.22*</u>	<u>0.22*</u>	<b>0.23</b>	0.24*	0.24*	<b>0.25</b>	0.26	0.27	0.28	<b>0.29</b>	1.00
21	<u>0.21</u>	<u>0.21</u>	<u>0.22*</u>	<u>0.22*</u>	<b>0.23</b>	0.24*	<b>0.25</b>	<b>0.25</b>	0.26	0.27	0.28	1.00
22	<u>0.21</u>	<u>0.21</u>	<u>0.21</u>	<u>0.22*</u>	<u>0.22*</u>	<b>0.23</b>	0.24*	<b>0.25</b>	0.26	0.27	0.28	1.00
23	0.20	<u>0.21</u>	<u>0.21</u>	<u>0.21</u>	<u>0.22*</u>	<b>0.23</b>	<b>0.23</b>	0.24*	<b>0.25</b>	0.26	0.27	1.00
24	0.20	0.20	0.20	<u>0.21</u>	<u>0.21</u>	<u>0.22*</u>	<b>0.23</b>	0.24*	0.24*	<b>0.25</b>	0.26	1.00
25	0.20	0.20	0.20	0.20	<u>0.21</u>	<u>0.22*</u>	<u>0.22*</u>	<b>0.23</b>	0.24*	<b>0.25</b>	0.26	1.00
26	<u>0.19</u>	<u>0.19</u>	0.20	0.20	0.20	<u>0.21</u>	<u>0.22*</u>	<u>0.22*</u>	<b>0.23</b>	0.24*	<b>0.25</b>	1.00
27	<u>0.19</u>	<u>0.19</u>	<u>0.19</u>	0.20	0.20	<u>0.21</u>	<u>0.21</u>	<u>0.22*</u>	<b>0.23</b>	0.24*	0.24*	1.00
28	<u>0.19</u>	<u>0.19</u>	<u>0.19</u>	<u>0.19</u>	0.20	0.20	<u>0.21</u>	<u>0.22*</u>	<u>0.22*</u>	<b>0.23</b>	0.24*	1.00
29	0.18	0.18	<u>0.19</u>	<u>0.19</u>	<u>0.19</u>	0.20	0.20	<u>0.21</u>	<u>0.22*</u>	<b>0.23</b>	<b>0.23</b>	1.00
30	0.18	0.18	0.18	<u>0.19</u>	<u>0.19</u>	<u>0.19</u>	0.20	<u>0.21</u>	<u>0.21</u>	<u>0.22*</u>	<b>0.23</b>	1.00
31	0.18	0.18	0.18	0.18	<u>0.19</u>	<u>0.19</u>	0.20	0.20	<u>0.21</u>	<u>0.22*</u>	<u>0.22*</u>	1.00
32	<u>0.17*</u>	<u>0.17*</u>	0.18	0.18	0.18	<u>0.19</u>	<u>0.19</u>	0.20	<u>0.21</u>	<u>0.21</u>	<u>0.22*</u>	1.00
33	<u>0.17*</u>	<u>0.17*</u>	<u>0.17*</u>	0.18	0.18	<u>0.19</u>	<u>0.19</u>	0.20	0.20	<u>0.21</u>	<u>0.21</u>	1.00
34	<u>0.17*</u>	<u>0.17*</u>	<u>0.17*</u>	<u>0.17*</u>	0.18	0.18	<u>0.19</u>	<u>0.19</u>	0.20	0.20	<u>0.21</u>	1.00
35	<u>0.17*</u>	<u>0.17*</u>	<u>0.17*</u>	<u>0.17*</u>	<u>0.17*</u>	0.18	0.18	<u>0.19</u>	<u>0.19</u>	0.20	<u>0.21</u>	1.00
36	<u>0.16</u>	<u>0.16</u>	<u>0.17*</u>	<u>0.17*</u>	<u>0.17*</u>	0.18	0.18	<u>0.19</u>	<u>0.19</u>	0.20	0.20	1.00
37	<u>0.16</u>	<u>0.16</u>	<u>0.16</u>	<u>0.17*</u>	<u>0.17*</u>	<u>0.17*</u>	0.18	0.18	<u>0.19</u>	<u>0.19</u>	0.20	1.00
38	<u>0.16</u>	<u>0.16</u>	<u>0.16</u>	<u>0.16</u>	<u>0.17*</u>	<u>0.17*</u>	0.18	0.18	<u>0.19</u>	<u>0.19</u>	0.20	1.00
39	<u>0.16</u>	<u>0.16</u>	<u>0.16</u>	<u>0.16</u>	<u>0.17*</u>	<u>0.17*</u>	<u>0.17*</u>	0.18	0.18	<u>0.19</u>	<u>0.19</u>	1.00
40	<u>0.16</u>	<u>0.16</u>	<u>0.16</u>	<u>0.16</u>	<u>0.16</u>	<u>0.17*</u>	<u>0.17*</u>	0.18	0.18	<u>0.19</u>	<u>0.19</u>	1.00
41	<u>0.15</u>	<u>0.15</u>	<u>0.16</u>	<u>0.16</u>	<u>0.16</u>	<u>0.16</u>	<u>0.17*</u>	<u>0.17*</u>	0.18	0.18	<u>0.19</u>	1.00
42	<u>0.15</u>	<u>0.15</u>	<u>0.15</u>	<u>0.16</u>	<u>0.16</u>	<u>0.16</u>	<u>0.17*</u>	<u>0.17*</u>	0.18	0.18	<u>0.19</u>	1.00
43	<u>0.15</u>	<u>0.15</u>	<u>0.15</u>	<u>0.15</u>	<u>0.16</u>	<u>0.16</u>	<u>0.16</u>	<u>0.17*</u>	<u>0.17*</u>	0.18	0.18	1.00
44	<u>0.15</u>	<u>0.15</u>	<u>0.15</u>	<u>0.15</u>	<u>0.16</u>	<u>0.16</u>	<u>0.16</u>	<u>0.17*</u>	<u>0.17*</u>	0.18	0.18	1.00
45	<u>0.15</u>	<u>0.15</u>	<u>0.15</u>	<u>0.15</u>	<u>0.15</u>	<u>0.16</u>	<u>0.16</u>	<u>0.16</u>	<u>0.17*</u>	<u>0.17*</u>	0.18	1.00
46	<u>0.15</u>	<u>0.15</u>	<u>0.15</u>	<u>0.15</u>	<u>0.15</u>	<u>0.15</u>	<u>0.16</u>	<u>0.16</u>	<u>0.17*</u>	<u>0.17*</u>	0.18	1.00
47	0.14	0.14	<u>0.15</u>	<u>0.15</u>	<u>0.15</u>	<u>0.15</u>	<u>0.16</u>	<u>0.16</u>	<u>0.16</u>	<u>0.17*</u>	<u>0.17*</u>	1.00

**Table 2** (continued)

$\sigma_N/\sigma_N^{(theo)} \quad 2b/q$	0	1	2	3	4	5	6	7	8	9	10	$\infty$
<b>48</b>	<u>0.14</u>	<u>0.14</u>	<u>0.14</u>	<b>0.15</b>	<b>0.15</b>	<b>0.15</b>	<b>0.15</b>	<b>0.16</b>	<b>0.16</b>	<b>0.17*</b>	<b>0.17*</b>	1.00
<b>49</b>	<u>0.14</u>	<u>0.14</u>	<u>0.14</u>	<u>0.14</u>	<b>0.15</b>	<b>0.15</b>	<b>0.15</b>	<b>0.16</b>	<b>0.16</b>	<b>0.16</b>	<b>0.17*</b>	1.00
<b>50</b>	<u>0.14</u>	<u>0.14</u>	<u>0.14</u>	<u>0.14</u>	<b>0.15</b>	<b>0.15</b>	<b>0.15</b>	<b>0.15</b>	<b>0.16</b>	<b>0.16</b>	<b>0.17*</b>	1.00
$\infty$	0.00	0.00	0.00	0.00	0.00	0.00	0.00	0.00	0.00	0.00	0.00	$(1+2a/b)^{-1}$

In **bold** type are represented the 15 different nanostrengths measured on single walled carbon nanotubes in bundle [7]; whereas in *italic* we report the 19 nanostrengths measured on multi walled carbon nanotubes [8], and in underlined type the most recent 18 observations [34]. All the data are reported with the exception of the five smallest values of 0.08, 0.10 [34], 0.11 [8], 0.12 [8, 34] and 0.13 [7], for which we would need for example adjacent vacancies ( $2b/q \sim 1$ ) in number  $n = 2a/q = 138-176$ ,  $90-109$ ,  $75-89$ ,  $64-74$  and  $55-63$  respectively. The 26 strengths measured in [38] are also treated (asterisks), simply assuming two interacting walls for  $100 < \sigma_N^{(exp)} \leq 200$  gigapascals (thus  $\sigma_N = \sigma_N^{(exp)}/2$ ) or 3 interacting walls for  $200 < \sigma_N^{(exp)} \leq 300$  gigapascals ( $\sigma_N = \sigma_N^{(exp)}/3$ ). All the experiments are referred to  $\sigma_N^{(theo)} = 100\text{GPa}$  ( $q \sim 0.25$  nm). If all the nanotubes in the cable contain identical holes,  $\sigma_C/\sigma_C^{(theo)} = \sigma_N/\sigma_N^{(theo)}$

where  $E_1 \approx 7$  eV is the energy required to remove one carbon atom and  $T_a$  is the absolute temperature at which the carbon is assembled, typically in the range between 2,000 and 4,000 K. Thus,  $f \approx 2.4 \times 10^{-18} - 1.6 \times 10^{-9}$ . For the megacable, having a carbon weigh of  $\sim 5,000$  kg, the total number of atoms is  $N \approx 2.5 \times 10^{29}$  thus a huge number of equilibrium defects, in the range  $n \approx 0.6 \times 10^{12} - 3.9 \times 10^{20}$  is expected, in agreement with a recent discussion [41] and observations [42].

The strength of the cable will be dictated by the largest transversal crack on it, according to the weakest link concept. The probability of finding a nanocrack of size  $m$  in a bundle with vacancy fraction  $f$  is  $P(m) = (1-f)^f m$ , and thus the number  $M$  of such nanocracks in a bundle composed by  $N$  atoms is  $M(m) = P(m)N^{27}$ . The size of the largest nanocrack, which typically occurs once, is found from the solution to the equation  $M(m) \approx 1$ , which implies [43]:

$$m \approx -\ln[(1-f)N]/\ln f \approx -\ln N/\ln f \quad (11)$$

Accordingly, we deduce a size  $m \approx 2-4$  for the largest thermodynamically unavoidable defect in the megacable. Inserting Eqs. 11 and 10 into Eq. 2 evaluated for a transversal crack ( $b \approx 0$  and  $2a/q \approx m$ ), we deduce the statistical counterpart of Eq. 2 and thus the following thermodynamical maximum achievable strength:

$$\frac{\sigma_N(N)}{\sigma_N^{(theo)}} \leq \frac{\sigma_N^{(max)}(N)}{\sigma_N^{(theo)}} = \frac{1}{\sqrt{1 + \frac{k_B T_a}{E_1} \ln N}} \quad (12)$$

Then, inserting Eq. 12 into Eqs. 3 and 4, the maximum cable strength and minimum taper-ratio can be statistically deduced. The corresponding maximum achievable

**Table 3** The new results [34] are here treated with respect to both strength and elasticity, assuming the presence of transversal nanocracks composed by  $n$  adjacent vacancies [4]

MWCNT number and fracture typology	Strength (GPa)	Young's modulus (GPa)	$\kappa$	$n$	$V$ (%)
1 (multiple load A)	8.2	1,100	1.01	148	0.07
2 (clamp failed)	10	840	0.98	100	0.23
3	12	680	1.00	69	0.44
4 (failure at the clamp)	12	730	0.98	69	0.40
5 (multiple load B)	14	1,150	1.02	51	0.14
6 (multiple load a)	14	650	0.97	51	0.62
7	15	1,200	1.05	44	0.11
8	16	1,200	1.02	39	0.13
9	17	960	1.00	34	0.49
10	19	890	0.97	27	0.74
11 (multiple load b)	21	620	0.99	22	1.51
12 (multiple load I)	21	1,200	0.99	22	0.22
13 (multiple load II)	23	1,250	0.99	18	0.17
14	30	870	1.00	11	1.92
15 (plasticity observed)	31	1,200	0.59 (0.99)	10	0.49
16 (plasticity observed)	34	680	0.69 (1.02)	8	3.80
17 (multiple load III)	41	1,230	1.03	5	0.69
18 (failure at the clamp)	66	1,100	0.98	2	4.90

The constitutive parameter  $\kappa$  has been estimated as  $\kappa \approx \ln(\varepsilon_N)/\ln(\sigma_N/E)$  for all the tests: note the low values for the two nanotubes that revealed plasticity (in brackets the values calculated up to the incipient plastic flow are also reported). The ideal strength is assumed to be of 100GPa and the theoretical Young's modulus of 1,300 GPa; by Eq. 2 the crack length  $n$  is calculated and introduced in Eq. 8 to derive the related vacancy fraction  $v$  ( $\xi = \pi/2$ )

Fracture in two cases was observed at the clamp; in one case the clamp itself failed, thus the deduced strength represents a lower bound of the nanotube strength. Three nanotubes were multiple loaded (in two a,b and A,B or in three I,II,III steps), i.e., after the breaking in two pieces of a nanotube, one of the two pieces was again tested and fractured at a higher stress. Two nanotubes displayed a plastic flow

A vacancy fraction of the order of few % is estimated, suggesting that such nanotubes are much more defective than as imposed by the thermodynamic equilibrium, even if the defects are small and isolated. However, note that other interpretations are still possible, e.g., assuming the nanotube is coated by an oxide layer and rationalizing the ratio between the observed Young's modulus and its theoretical value as the volumetric fraction (for softer coating layers) of carbon in the composite structure

strength, an unavoidable limit (at least at the thermodynamic equilibrium), is  $\sim 45$  GPa and the corresponding flaw-tolerant taper-ratio is  $\sim 4.6$ . But the larger taper-ratio implies a large cable mass and thus a large number  $N$  of atoms. Updating  $N$  in our statistical calculation yields the same, thus self-consistent, predictions. Statistically we expect and even smaller strength, as previously discussed.



## Conclusions

The strength of a real, thus defective, carbon nanotube macroscopic cable is expected to be strongly reduced with respect to the theoretical strength of a carbon nanotube. Accordingly, in this chapter key simple formulas for the design of nanotube bundles (e.g. the space elevator megacable) have been reported.

## References

1. Y.V. Artsutanov, Kosmos na Elektrovoze, Komsomol-skaya Pravda, July 31 (1960); contents described in Lvov, V. Science **158**, 946–947 (1967)
2. J. Pearson, The orbital tower: a spacecraft launcher using the Earth's rotational energy. Acta Astronaut. **2**, 785–799 (1975)
3. N. Pugno, On the strength of the nanotube-based space elevator cable: from nanomechanics to megamechanics. J. Phys. Condens. Matter **18**, S1971–S1990 (2006)
4. N. Pugno, The role of defects in the design of the space elevator cable: from nanotube to megatube. Acta Mater. **55**, 5269–5279 (2007)
5. N. Pugno, Space elevator: out of order? Nano Today **2**, 44–47 (2007)
6. S. Iijima, Helical microtubules of graphitic carbon. Nature **354**, 56–58 (1991)
7. M.F. Yu, B.S. Files, S. Arepalli, R. Ruoff, Tensile loading of ropes of single wall carbon nanotubes and their mechanical properties. Phys. Rev. Lett. **84**, 5552–5555 (2000)
8. M.F. Yu, O. Lourie, M.J. Dyer, K. Moloni, T.F. Kelly, R. Ruoff, Strength and breaking mechanism of multiwalled carbon nanotubes under tensile load. Science **287**, 637–640 (2000)
9. B.C. Edwards, Design and deployment of a space elevator. Acta Astronaut. **10**, 735–744 (2000)
10. B.C. Edwards, E.A. Westling, *The Space Elevator: A Revolutionary Earth-to-Space Transportation System* (Spaseo Inc., San Francisco, CA, 2003)
11. N. Pugno, A quantized Griffith's criterion, Fracture Nanomechanics, Meeting of the Italian Group of Fracture, Vigevano, Italy, 25–26 Sept 2002
12. N. Pugno, R. Ruoff, Quantized fracture mechanics. Phil. Mag. **84**, 2829–2845 (2004)
13. N. Pugno, Dynamic quantized fracture mechanics. Int. J. Fract. **140**, 158–168 (2006)
14. N. Pugno, New quantized failure criteria: application to nanotubes and nanowires. Int. J. Fract. **141**, 311–328 (2006)
15. N. Pugno, F. Borgia, A. Carpinteri, Multiscale stochastic simulations as in-silico tensile testing of nanotube-based megacables. Small **4**, 1044–1052 (2008)
16. N. Pugno, R. Ruoff, Nanoscale Weibull statistics. J. Appl. Phys. **99**, 1–4 (2006)
17. A. Carpinteri, Scaling laws and renormalization groups for strength and toughness of disordered materials. Int. J. Solid Struct. **31**, 291–302 (1994)
18. A. Carpinteri, N. Pugno, Are the scaling laws on strength of solids related to mechanics or to geometry? Nat. Mater. **4**, 421–423, (2005)
19. N. Pugno, A general shape/size-effect law for nanoindentation. Acta Mater. **55**, 1947–1953 (2007)
20. M. Ippolito, A. Mattoni, L. Colombo, N. Pugno, The role of lattice discreteness on brittle fracture: how to reconcile atomistic simulations to continuum mechanics. Phys. Rev. B **73**, 104111–1/6 (2006)
21. D. Taylor, P. Cornetti, N. Pugno, The fracture mechanics of finite crack extensions. Eng. Fract. Mech. **72**, 1021–1028 (2005)
22. N. Pugno, M. Ciavarella, P. Cornetti, A. Carpinteri, A unified law for fatigue crack growth. J. Mech. Phys. Solid. **54**, 1333–1349 (2006)
23. N. Pugno, P. Cornetti, A. Carpinteri, New unified laws in fatigue: from the Wöhler's to the Paris' regime. Eng. Fract. Mech. **74**, 595–601 (2007)

24. J.R. Rice, G.F. Rosengren, Plane strain deformation near a crack tip in a power-law hardening material. *J. Mech. Phys. Solid.* **16**, 1–12 (1968)
25. A. Carpinteri, N. Pugno, Fracture instability and limit strength condition in structures with re-entrant corners. *Eng. Fract. Mech.* **72**, 1254–1267 (2005)
26. A. Carpinteri, B. Chiaia, Crack-resistance behavior as a consequence of self-similar fracture topologies. *Int. J. Fract.* **76**, 327–340 (1996)
27. Q.Z. Wang, Simple formulae for the stress-concentration factor for two- and three-dimensional holes in finite domains. *J. Strain Anal.* **73**, 259–264 (2002)
28. N. Pugno, Young's modulus reduction of defective nanotubes. *Appl. Phys. Lett.* **90**, 043106 (2007)
29. N. Pugno, H. Troger, A. Steindl, M. Schwarzbart, On the stability of the track of the space elevator. Proceedings of the 57th international astronautical congress, Valencia, Spain, 2–6 October 2007
30. S.L. Mielke, D. Troya, S. Zhang, J.-L. Li, S. Xiao, R. Car, R.S. Ruoff, G.C. Schatz, T. Belytschko, The role of vacancy defects and holes in the fracture of carbon nanotubes. *Chem. Phys. Lett.* **390**, 413–420 (2004)
31. T. Belytschko, S.P. Xiao, R. Ruoff, Effects of defects on the strength of nanotubes: experimental-computational comparisons, Los Alamos National Laboratory, Preprint Archive, Physics, arXiv:physics/0205090 (2002)
32. S. Zhang, S.L. Mielke, R. Khare, D. Troya, R.S. Ruoff, G.C. Schatz, T. Mechanics of defects in carbon nanotubes: atomistic and multiscale simulations. *Phys. Rev. B* **71**, 115403 1–12 (2005)
33. R. Khare, S.L. Mielke, J.T. Paci, S. Zhang, R. Ballarini, G.C. Schatz, T. Belytschko, Coupled quantum mechanical/molecular mechanical modelling of the fracture of defective carbon nanotubes and grapheme sheets. *Phys. Rev. B* **75**, 075412 (2007)
34. W. Ding, L. Calabri, K.M. Kohlhaas, X. Chen, D.A. Dikin, R.S. Ruoff, Modulus, fracture strength, and brittle vs. plastic response of the outer shell of arc-grown multiwalled carbon nanotubes. *Exp. Mech.* **47**, 25–36 (2006)
35. M. Meo, M. Rossi, Tensile failure prediction of single wall carbon nanotube. *Eng. Fract. Mech.* **73**, 2589–2599 (2006)
36. M. Sammalkorpi, A. Krashennnikov, A. Kuronen, K. Nordlund, K. Kaski, Mechanical properties of carbon nanotubes with vacancies and related defects. *Phys. Rev. B* **70**, 245416–1/8 (2004)
37. W. Weibull, *A Statistical Theory of the Strength of Materials* (Ingeniörsvetenskapsakademiens, Handlingar, 1939), p. 151
38. A.H. Barber, I. Kaplan-Ashiri, S.R. Cohen, R. Tenne, H.D. Wagner, Stochastic strength of nanotubes: an appraisal of available data. *Compos. Sci. Tech.* **65**, 2380–2386 (2005)
39. I. Kaplan-Ashiri, S.R. Cohen, K. Gartsman, V. Ivanovskaya, T. Heine, G. Seifert, I. Wiesel, H.D. Wagner, R. Tenne, On the mechanical behavior of WS<sub>2</sub> nanotubes under axial tension and compression. *Proc. Natl. Acad. Sci. U.S.A.* **103**, 523–528 (2006)
40. C. Kittel, *Introduction to Solid State Physics* (John Wiley & Sons, New York, 1966)
41. H.K.D.H. Bhadeshia, 52nd Hatfield Memorial Lecture – Large chunks of very strong steel. *Mater. Sci. Tech.* **21**, 1293–1302 (2005)
42. Y. Fan, B.R. Goldsmith, P.G. Collins, Identifying and counting point defects in carbon nanotubes. *Nat. Mater.* **4**, 906–911 (2005)
43. P.D. Beale, D.J. Srolovitz, Elastic fracture in random materials. *Phys. Rev. B* **37**, 5500–5507 (1988)